polysaccharides

MDPI

Article

Development and Investigation of Zein and Cellulose Acetate Polymer Blends Incorporated with Garlic Essential Oil and β-Cyclodextrin for Potential Food Packaging Application

Clara Suprani Marques [1,*], Rafael Resende Assis Silva [2], Tarsila Rodrigues Arruda [1], Ana Luiza Valadares Ferreira [1], Taíla Veloso de Oliveira [1], Allan Robledo Fialho Moraes [3], Marali Vilela Dias [4], Maria Cristina Dantas Vanetti [5] and Nilda de Fátima Ferreira Soares [1]

[1] Food Technology Department, Federal University of Viçosa, Viçosa 36570-900, Brazil; tarsila.arruda@ufv.br (T.R.A.); ana.valadares@ufv.br (A.L.V.F.); taila.oliveira@ufv.br (T.V.d.O.); nfsoares10@gmail.com (N.d.F.F.S.)
[2] Department of Materials Science and Engineering, Federal University of São Carlos, São Carlos 13565-905, Brazil; rafaelras@estudante.ufscar.br
[3] Agricultural Science Institute, Federal University of Viçosa, Rio Paranaiba 38810-000, Brazil; allan.moraes@ufv.br
[4] Department of Food Science, Federal University of Lavras, Lavras 37200-900, Brazil; maralivileladias@gmail.com
[5] Department of Microbiology, Federal University of Viçosa, Viçosa 36570-900, Brazil; mvanetti@ufv.br
* Correspondence: supraniclara@mail.com

check for updates

Citation: Marques, C.S.; Silva, R.R.A.; Arruda, T.R.; Ferreira, A.L.V.; Oliveira, T.V.d.; Moraes, A.R.F.; Dias, M.V.; Vanetti, M.C.D.; Soares, N.d.F.F. Development and Investigation of Zein and Cellulose Acetate Polymer Blends Incorporated with Garlic Essential Oil and β-Cyclodextrin for Potential Food Packaging Application. *Polysaccharides* **2022**, *3*, 277–291. https://doi.org/10.3390/polysaccharides3010016

Academic Editor: Rajkumar Patel

Received: 30 January 2022
Accepted: 6 March 2022
Published: 12 March 2022

Abstract: The obtainment of new materials with distinct properties by mixing two or more polymers is a potential strategy in sustainable packaging research. In the present work, a blend of cellulose acetate (CA) and zein (60:40 wt/wt CA:zein) was manufactured by adding glycerol or tributyrin as plasticizers (30% wt/wt), and garlic essential oil (GEO), complexed (IC) or not with β-cyclodextrin (βCD), to produce active packaging. Blends plasticized with tributyrin exhibited a more homogeneous surface than those containing glycerol, which showed major defects. The blends underperformed compared with the CA films regarding mechanical properties and water vapor permeability. The presence of IC also impaired the films' performance. However, the blends were more flexible than zein brittle films. The films added with GEO presented in vitro activity against *Listeria innocua* and *Staphylococcus aureus*. The IC addition into films, however, did not ensure antibacterial action, albeit that IC, when tested alone, showed activity against both bacteria. These findings suggest that the mixture of CA and plasticizers could increase the range of application of zein as a sustainable packaging component, while essential oils act as a natural bioactive to produce active packaging.

Keywords: active packaging; bio-based polymer; cellulose acetate; essential oils; food packaging; inclusion complex; zein

1. Introduction

Plastics revolutionized the food packaging sector since they are available at low cost, flexible, durable, versatile, and have distinct mechanical and barrier properties, suitable for food preservation [1,2]. However, the rampant consumption and improper disposal of plastics has resulted in a worldwide problem, causing damage to the environment and human health. In order to reduce the manufacture and use of materials from nonrenewable sources, various strategies are proposed, such as recycling and the total or partial replacement of conventional plastics with bio-based materials [2–9].

Derived from several renewable sources (i.e., agroindustrial byproducts and feedstock), bio-based materials have become increasingly popular among researchers from the packaging area since they fulfill the requirements for sustainable development [2,10]. In this context, several bio-based polymers extracted from different sources have been

investigated as potential compounds for packaging. Cellulose derivatives, such as CA, and plant proteins, such as zein, are examples of hydrophobic polymers of natural origin that are already approved by the FDA to be used as food contact substances (CA) or listed as GRAS (zein) [4,11–13].

However, despite the growing trend, studies have revealed that films elaborated with bio-based polymers leave much to be desired when compared with the petroleum-based ones. Regarding food packaging and its role in food preservation, the higher water vapor permeability and lower mechanical properties that bio-based films usually present may impair their application as packaging components [2,10]. Aiming at improving the polymers' performance as a packaging material, several strategies are considered.

The blend or mixture of two or more polymers for obtaining a new material with distinct characteristics is one of these proposed strategies [14,15]. The incorporation of different additives can also allow the elaboration of films with improved properties and/or functions [4,5,16–18]. Plasticizers, such as glycerol, for example, are widely used since they can enhance films' flexibility. They are usually low-molecular weight compounds with low or no volatility, and able to increase polymer chain mobility [16,17].

Essential oils (EOs) are another example of additives for food packaging due to their bioactive properties and natural appeal. Some EOs show antimicrobial activity, which could grant to the packaging a preservative action, contributing to food safety and shelf-life extension [5,6,19,20]. However, the direct incorporation of EOs into polymer matrices is not recommended due to several issues (EOs are prone to thermal and light degradation, for instance) [21]. Thus, their complexation with cyclodextrins (CDs), followed by their addition into polymeric matrices, is considered an interesting way to protect the EOs' active compounds from the degradation caused by light, temperature exposure, and oxygen presence, as well as to minimize their sensorial impact [18]. βCD, for example, is a low-cost natural CD recognized as safe and already used in food items and drugs [18–20].

Within this context, the present work aimed to obtain, characterize, and compare blends of CA and zein with two different plasticizers, glycerol and tributyrin. Although CA:zein blends have already been studied as nanofibers in the biomedical area, their potential as a food packaging material is not elucidated in the literature [22,23]. In addition, GEO was added into the films, free or as an inclusion complex (IC) with βCD, aiming at elaborating active films with antibacterial action. Two hypotheses were investigated: (1) that there would be an improvement in the properties of the new material compared with those of the individual polymers; and (2) that the incorporation of the EO in the complexed form would ensure a better antibacterial action by the films when compared with the ones with added non-complexed EO.

2. Materials and Methods

2.1. Materials

CA (SD = 2.5, and average molar mass of 2,024,000 g·mol^{-1}) was donated by Rhodia Solvay Group (São Paulo, Brazil). Zein was donated by Flo Chemical Corp (F4400, molecular mass of 15–26 kDa) (Ashburnham, MA, USA). Glycerol (LabSynth, Diadema, Brazil) and tributyrin (98% purity degree, Acros Organics, Mumbai, India) were the plasticizers investigated. Anhydrous ethanol (99.8% purity degree, Neon, Brazil) and acetone (99.5% purity degree, LabSynth, Brazil) were the solvents used for polymer dispersion. GEO suitable for food was purchased from Empório Laszlo (Brazil), and βCD (97% purity degree) was acquired from Sigma-Aldrich (Saint Louis, MO, USA).

2.2. Preparation of Geo:βCD Inclusion Complex

IC was prepared using a kneading method following the mass proportion of 88% of βCD and 12% of GEO [19], which approximately matches the 1:1 molar ratio when considering the GEO compound's average molar mass. The IC preparation was performed according to the methodology of Marques et al. [20], with modifications. In a porcelain mortar, 880 mg of βCD was added to 880 µL of hydroalcoholic solution (1:3 v/v ethanol:water)

and homogenized for 5 min. Subsequently, 120 mg of GEO was added to the obtained paste and the mixture was manually macerated for up to 30 min. Samples were dried in a desiccator containing silica gel for 48 h at 25 °C, ground, and stored. A physical mixture (PM) was prepared for comparison purposes by briefly mixing 880 mg of βCD and 120 mg of GEO in a mortar.

2.3. Characterization of Inclusion Complex

2.3.1. Entrapment Efficiency (EE%)

Determination of GEO amounts in the IC was performed spectrophotometrically according to the method of Hill, Gomes, and Taylor [24] with modifications. Initially, a calibration curve was obtained from GEO solutions ranging from 0.0010 μL·mL^{-1} to 0.0088 μL·mL^{-1} in isopropanol:acetonitrile (3:2 v/v) at 209 nm of UV absorbance (UV1800, Shimadzu, Japan). 20 mg of ICs samples was dispersed in 20 mL of isopropanol:acetonitrile and mixed for 48 h. After this, samples were centrifuged at 3200× g (model 4K-15, Sigma, Postfch, Germany), for 15 min. The supernatant was measured at 209 nm of UV absorbance. The percentage of GEO entrapped in ICs was calculated using Equation (1):

$$EE\% = \frac{GEO_R}{GEO_T} \times 100 \quad (1)$$

in which GEO_R and GEO_T represent the real and the theoretical amounts of GEO entrapped in the IC, respectively.

2.3.2. Thermal Stability

Thermogravimetric analysis (TGA) was performed on a thermogravimetric analyzer, (Model DTG-60H, Shimadzu, Japan), under a nitrogen atmosphere (50 mL·min^{-1}). Approximately 3 mg of each sample was weighed and heated from 25 °C to 360 °C at a rate of 10 °C·min^{-1}. TG curves were obtained for βCD, IC, PM, and GEO.

The thermal stability of the elaborated films and their components was verified as well. The parameters were the same, with the exception of the final temperature, which was 550 °C.

2.3.3. X-ray Diffraction (XRD)

X-ray diffractograms for βCD, IC, and PM were obtained through a BRUKER X-ray diffractometer (model D8 Discover) equipped with an X-ray tube (Cu-Kα radiation, λ = 0.1514 nm), in a 2θ range from 5° to 70° with a scanning rate of 0.05° s^{-1}.

2.4. Elaboration of Polymer Blends

Aiming to obtain a CA:zein blend, each polymer was, at first, dispersed separately. CA was dispersed in acetone (1:10 wt/v) and allowed to rest for 24 h. Zein was dispersed in ethanol 80% (v/v), at a ratio of 1:10 (wt/v), stirring at 500 rpm at 65 °C for 10 min. After they had cooled back to room temperature (approximately 25 °C), the dispersions were mixed together following the proportion of 60:40 CA:zein (wt/wt), since previous tests conducted in the laboratory revealed that this ratio allowed the obtainment of a more homogeneous film when compared with the others (Figure S1 of Supplementary Material). The plasticizer (glycerol or tributyrin) was also added to the mixed dispersion in a proportion of 30% (wt/wt) based on the polymer mass, as well as the bioactive agents: GEO (10% wt/wt) or IC (10% wt/wt), also based on the polymer mass. The dispersion was homogenized at 5000 rpm for 2 min (model T25, Ultra Turrax, IKA), allowed to rest for 30 min, poured onto a glass plate with machine casting (K-Paint applicator, Litlington, Royston, Hertfordshire, UK), and allowed to dry at room temperature. A blend without a bioactive agent and a blend containing 10% βCD were also investigated as control samples. Therefore, four different blends and four CA-films for each plasticizer were obtained, resulting in 16 assays, as described in Table 1. For comparison purposes, films with only CA and only zein were elaborated as well (Figure S2 of Supplementary Material).

Table 1. Elaborated films with different plasticizers and additives: cellulose acetate and zein blends (BL) (ratio 60:40 CA:zein wt/wt) and their respective cellulose-acetate-based controls (CA).

Sample	Plasticizer (30% wt/wt)	Additive (10% wt/wt)
BL-T-CNT	Tributyrin	-
BL-T- βCD	Tributyrin	β-cyclodextrin
BL-T-GEO	Tributyrin	Garlic essential oil
BL-T-IC	Tributyrin	Inclusion complex
CA-T-CNT	Tributyrin	-
CA-T- βCD	Tributyrin	β-cyclodextrin
CA-T-GEO	Tributyrin	Garlic essential oil
CA-T-IC	Tributyrin	Inclusion complex
BL-G-CNT	Glycerol	-
BL-G- βCD	Glycerol	β-cyclodextrin
BL-G-GEO	Glycerol	Garlic essential oil
BL-G-IC	Glycerol	Inclusion complex
CA-G-CNT	Glycerol	-
CA-G- βCD	Glycerol	β-cyclodextrin
CA-G-GEO	Glycerol	Garlic essential oil
CA-G-IC	Glycerol	Inclusion complex

2.5. Characterization of Polymer Blends

2.5.1. Scanning Electron Microscopy

Micrographs of films' surface and films' cross-sectional area, after liquid-nitrogen brittle fracture, were obtained with a scanning electron Tabletop Microscope (model TM3000, Hitachi High-Technologies, Tokyo, Japan) with a secondary electron detector and operating under low vacuum. Uncoated samples were attached to stubs' surface with a double-sided carbon tape aid, and the accelerating voltage of 15 KV was used.

2.5.2. Thickness and Mechanical Properties

Film thickness was measured, in μm, with a digital micrometer (model 547–401, Mitutoyo, Japan). Ten specimens of each treatment were analyzed at ten random points per sample [5]. The films' mechanical properties were also evaluated; factors analyzed were tensile strength (TS, in MPa), elongation at break (E, in %), and modulus of elasticity (Young's modulus, YM, in MPa) using a Universal Testing Machine (model 3367, Instron Corporation, USA) equipped with a 1 kN load cell. Five rectangular specimens of each treatment (175 mm × 25 mm) were tested. The initial distance of grids' separation was 125 mm, and the rate of separation was 50 mm·min^{-1} [25].

2.5.3. Water Vapor Permeability (WVP)

WVP was investigated by the gravimetric method according to ASTM E96/E96M (2010) [26] (with a few modifications), which allowed the calculation of the water vapor transmission rate (WVTR) as a function of weight gain. The films were cut into circles (Ø = 83 mm) and sealed with parafilm in poly(methyl methacrylate) cups containing a saturated solution of lithium chloride (12 ± 5% RH at 25 ± 2 °C). After this, the cups were placed in desiccators containing a saturated solution of sodium chloride (75 ± 5% RH at 25 ± 2 °C). The cups were periodically weighted to provide at least ten data points. Graphs expressing the gain of mass over time allowed the determination of the WVTR according to Equation (2):

$$\mathrm{WVTR} = \frac{\mathrm{m}}{\mathrm{t}\cdot\mathrm{A}} \quad (2)$$

in which m/t is the slope of gain of mass (g) over time (h), and A is the permeation area (m^2). After this, the WVP was obtained according to Equation (3):

$$\mathrm{WVP} = \frac{\mathrm{WVTR}\cdot X_T}{P_S\cdot(RH_1 - RH_2)} \quad (3)$$

in which X_T is the film thickness, P_S is the saline water saturation pressure, RH_1 is the relative humidity in the desiccator containing NaCl, and RH_2 is the relative humidity on the desiccator containing LiCl. WVP was expressed as $g \cdot Pa^{-1} \cdot s^{-1} \cdot m^{-1}$.

2.6. Investigation of Antibacterial Properties

The antibacterial activity of GEO was initially investigated against Gram-positive bacteria *Staphylococcus aureus* ATCC 6538 and *Listeria innocua* ATCC 33090, and Gram-negative bacteria *Escherichia coli* ATCC 11229, *Pseudomonas fluorescens* 0A7, and *Salmonella* Choleraesuis ATCC 10708 Since the EO only showed activity against the Gram-positive bacteria, *L. innocua* and *S. aureus* were used for investigation of minimal inhibitory concentrations of GEO and IC, as well as for evaluation of the films. *P. fluorescens* was selected as negative control.

2.6.1. Inocula Preparation

Selected colonies of the bacteria were taken from a non-selective medium (plate count agar, PCA, Oxoid, Basingstoke, Hampshire, England) and were suspended in 0.85% (m/v) saline solution until they reached a visual suspension density similar to 0.5 McFarland turbidity standard (around 1–2 $\times$ 10^7 $CFU \cdot mL^{-1}$), then diluted at 1:10 [22].

2.6.2. Minimal Inhibitory Concentration (MIC)

The agar dilution method, with a few modifications, was used to investigate the MIC of GEO and IC [27]. Samples of both bioactive agents were dispersed in 10 mL of liquefied Brain Heart Infusion (BHI, Himedia, India) agar (~45 °C), resulting in the final concentrations of 2650 $\mu g \cdot mL^{-1}$, 1272 $\mu g \cdot mL^{-1}$, 636 $\mu g \cdot mL^{-1}$, 318 $\mu g \cdot mL^{-1}$, 159 $\mu g \cdot mL^{-1}$, 79.5 $\mu g \cdot mL^{-1}$, and 39.75 $\mu g \cdot mL^{-1}$ for GEO, and 9600 $\mu g \cdot mL^{-1}$, 4800 $\mu g \cdot mL^{-1}$, 2400 $\mu g \cdot mL^{-1}$, 1200 $\mu g \cdot mL^{-1}$, 600 $\mu g \cdot mL^{-1}$, and 300 $\mu g \cdot mL^{-1}$ for IC. Negative controls were BHI agar and BHI agar with 9600 $\mu g \cdot mL^{-1}$ of βCD. After allowing the agar to set and solidify, aliquots of 20 µL of the inoculum (Section 2.6.1) were dispensed on the dried agar surface, resulting in a final bacterial concentration of approximately 10^4 $CFU \cdot mg^{-1}$ per spot. The plates were incubated at 37 ± 1 °C for 24 h. MIC was determined based on the lowest concentration capable of growth inhibition.

2.6.3. Film Antibacterial Activity by Indirect Contact

The elaborated films were cut into (2 $\times$ 4) cm^2 shapes and fixed onto the lids of Petri dishes. The plates were previously prepared with BHI agar and inoculated with *S. aureus* or *L. innocua* (Section 2.6.1) with a swab aid [6]. The incubation conditions were 24 h at 37 °C ± 1 °C (*S. aureus* and *L. innocua*) and 10 days at 7 °C ± 1 °C (*L. innocua*). The presence or absence of microbial growth was evaluated after the incubation period.

2.7. Statistical Analysis

Analysis of variance (ANOVA) was carried out and followed by Tukey's test at 5% probability, if suitable. The statistical software R was used [28].

3. Results and Discussion

3.1. Inclusion Complex Characterization

The IC preparation of GEO with βCD was achieved by the kneading method, which was chosen due to the practicality and quality of the technique [20,29]. To calculate the GEO entrapped in ICs, the calibration curve was obtained (Equation (4)) with an adjusted R^2 of 0.9942.

$$Y_{209\ nm} = 0.0299 + 69.052X_{GEO} \quad (4)$$

in which Y_{209} is the measured absorbance at 209 nm and X_{GEO} is the EO concentration. The entrapment efficiency calculated was 87.5%.

The thermogravimetric curves, as well as their derivatives, plus the X-ray diffractograms of IC and pristine materials are displayed in the Supplementary Material,

Figures S3 and S4, respectively. Regarding the thermal analyses, the βCD mass losses, exhibited in the TG curve, occurred in two steps: at 25–120 °C, losing 12.6%, due to water loss, and above 309 °C, corresponding to 76.7% of material decomposition, corroborating with Giordano et al. [30]. The EO mass loss displayed in the GEO TG curve started at room temperature (~25 °C) and achieved around 95% of loss until 200 °C. A similar behavior was observed by Piletti et al. [31] when studying the thermal protection of complexed GEO.

Three stages were observed for the TG curve of PM: at 25–120 °C, losing 14.5%, at 120–250 °C (4.0%), and above 300 °C, with 66.2% of material degradation. In the first and second stages, PM exhibited an intermediary behavior between βCD and GEO mass loss under temperature increase. The initial mass loss of the PM system was higher than that of the βCD system, which may have occurred due to water molecule loss besides non-complexed EO volatilization.

The IC TG curve, in turn, presented an initial mass loss of 7%, a lower value than that verified for βCD and PM. This occurrence is discussed in the literature as an indication that the complexation was successfully achieved [31,32]. It can also be observed that ~5% IC mass loss occurred at 100–250 °C, which can be attributed to the degradation of non-complexed EO [20,31]. The material degradation occurred near 300 °C, with 62% of mass loss. A small peak, slightly before material degradation, can be observed in the IC DTG curve, emphasized by a red arrow in Figure S3. This can be attributed to complexed GEO volatilization, which occurred at a higher temperature than for non-complexed GEO, indicating greater thermal stability of the IC compound [31].

Regarding the XRD analyses (Figure S4), the βCD diffractogram exhibited the characteristic peaks for βCD at 2θ = 9.0°, 12.4°, 16.9°, 22.6°, 27.1°, 31.9°, 34.6°, and 35.5° [33]. The PM diffractogram presented peaks similar to those of βCD, albeit at a lesser intensity. On the other hand, in the IC diffractogram, it is possible to observe greater changes in the XDR profile, such as broadening, appearance, and disappearance of some peaks [20,32]. The decrease in the degree of crystallinity, as can be observed when comparing the IC diffractogram with βCD and PM diffractograms, with the disappearance of some well-defined and narrow peaks (pointed out with black arrows in Figure S4), can be a result of changes that occurred in the βCD's molecular organization, an indicative that the complexation with GEO was achieved [32,34].

3.2. Polymer Blends Aspect

The manufactured CA:zein blends and the CA-films incorporated with tributyrin or glycerol as plasticizers and the additives (GEO, IC, or βCD) are displayed in Figure 1. The blends presented a yellowish color and a porous appearance when compared with the transparent CA films, probably due to the zein addition (Figure 1 and Figure S2). The films' aspect also changed as a function of the type of plasticizer used. Tributyrin incorporation resulted in blends with a more homogeneous surface than blends with added glycerol, which in turn presented serious defects.

In addition, SEM micrographs revealed the presence of micro-sized globules in the cross-sectional areas of blends with added glycerol, which were not observed in blends with added tributyrin, suggesting a poor compatibility between glycerol and the polymers (Figure 2). Tributyrin is a triglyceride of butyric acid which is more hydrophobic than glycerol, and since both polymers (CA and zein) used have a more hydrophobic nature, the obtained result is coherent [35]. The incorporation of βCD or IC into blends or CA films also resulted in major changes in films' appearance and thickness, exhibiting more irregular surfaces than the control samples and the ones containing GEO. The presence of lumps and aggregates indicates poor compatibility among these additives and the polymers.

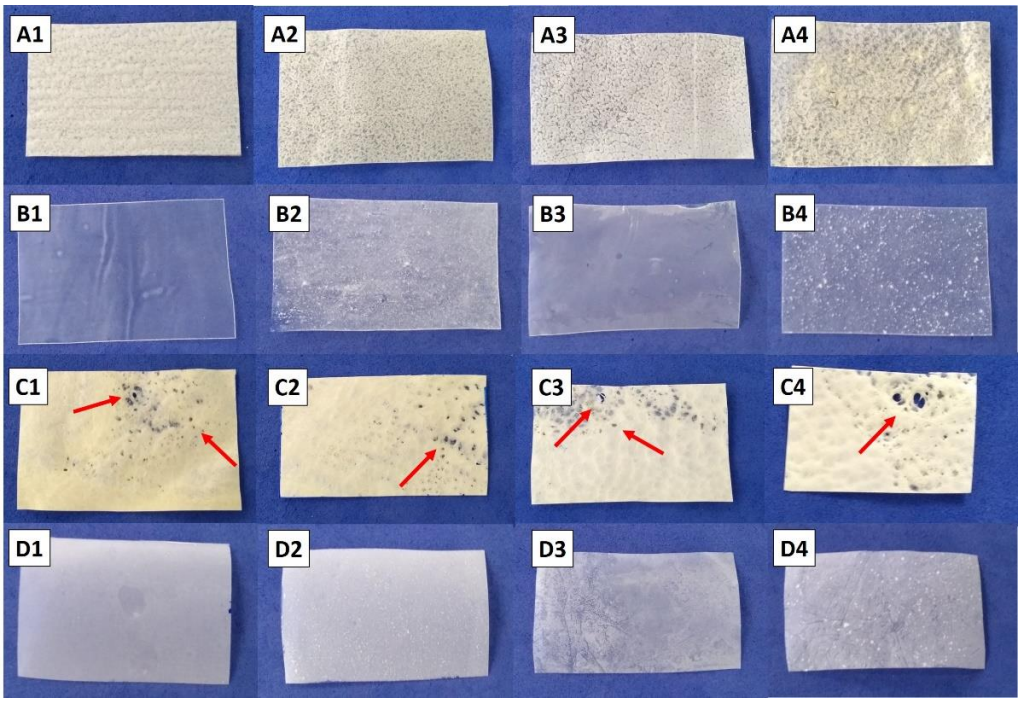

Figure 1. Images of the obtained blends and cellulose acetate (CA) films. Blends (line A) and their respective CA films (line B) with incorporated tributyrin and additives: control (no additive, **A1**,**B1**), βCD (**A2**,**B2**), GEO (**A3**,**B3**), and inclusion complex (**A4**,**B4**). Blends (line C) and their respective CA films (line D) with incorporated glycerol and additives: control (no additive, **C1**,**D1**), βCD (**C2**,**D2**), GEO (**C3**,**D3**), and inclusion complex (**C4**,**D4**). Red arrows indicate the presence of macro-holes and tears.

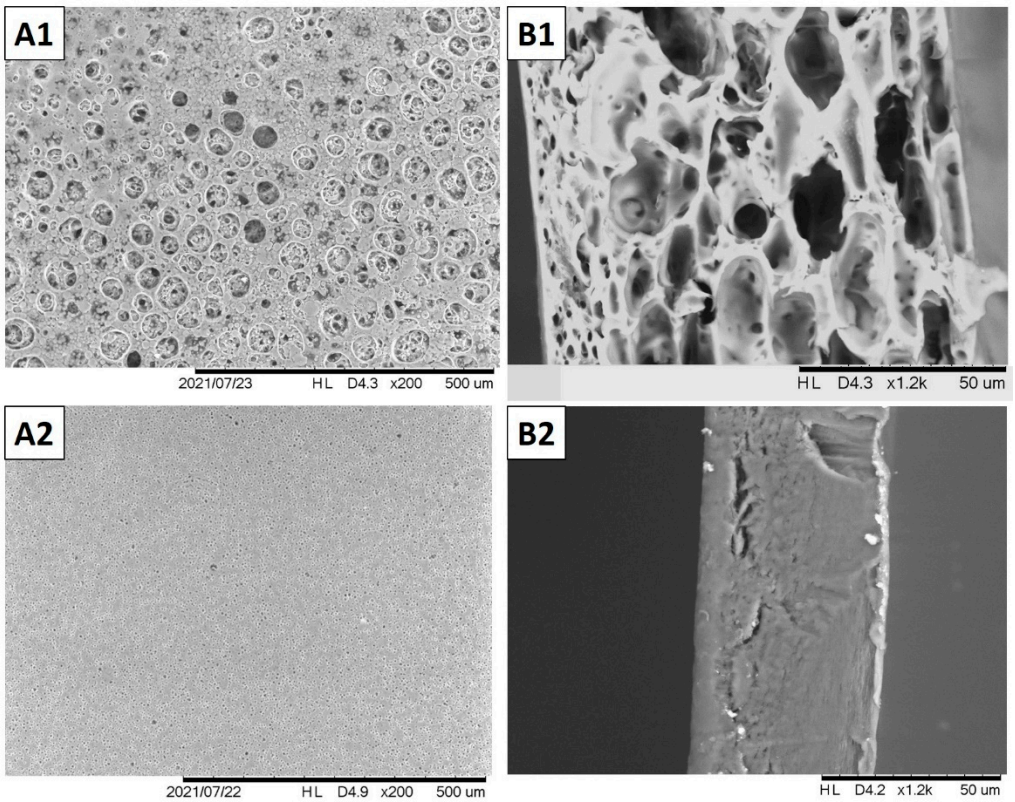

Figure 2. *Cont.*

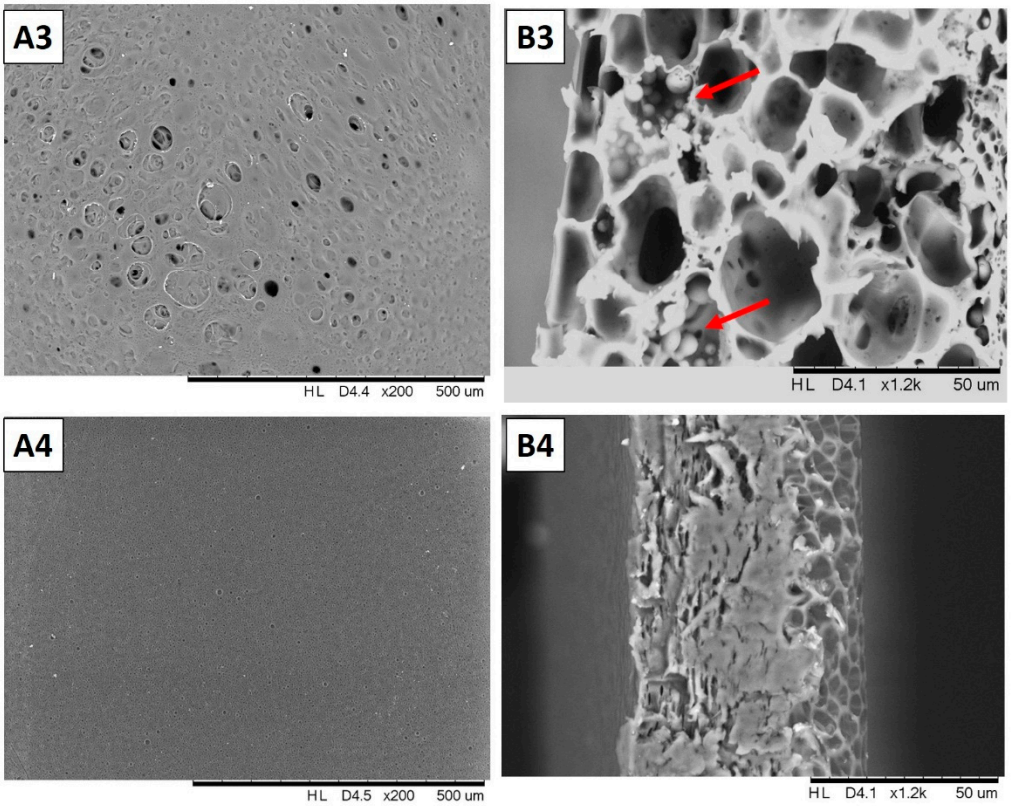

Figure 2. Scanning Electron micrographs of surface (**A**) and cross-section (**B**) of blends and cellulose acetate (CA) films. CA:zein blend with incorporated tributyrin (**A1**,**B1**); CA film with tributyrin (**A2**,**B2**); CA:zein blend with incorporated glycerol (**A3**,**B3**), and CA film with glycerol (**A4**,**B4**). Red arrows show glycerol micro-globules.

3.3. Thermogravimetric Analysis

The results obtained from the thermal analysis support the ones observed in the SEM micrographs. TG curves and their respective derivatives of pure materials, CA films, and CA:zein blends are displayed in Figure 3. Moreover, TG curves and their derivatives of all 16 films can be found in the Supplementary Material (Figure S5).

Both plasticizers lost approximately 100% of their mass close to 200 °C. Regarding the polymers, CA and zein exhibited loss of around 3% of their mass at 100 °C due to water molecule loss [36]. The peak-temperature degradation was 320 °C and 360 °C for zein and CA, respectively. A physical mixture (PM) of zein and CA was also prepared and investigated. In the DTG curve, it is possible to distinguish two peaks in the range of 320–360 °C (Figure 3-1B), indicating that the degradation of each polymer occurred separately from the other. In contrast, when observing the DTG curves of the blends (Figure 3-2B), a single peak around 350 °C is verified for the blend with added tributyrin, while a slight double peak can be seen in the DTG of the blend with added glycerol. This observation is a possible indication that the zein–CA–tributyrin compatibility was higher than the zein–CA–glycerol compatibility. Both CA films and blends containing tributyrin lost mass slower than those plasticized with glycerol, and the mass losses matched around 240 °C. Films plasticized with tributyrin exhibited only two stages of mass loss (plasticizer degradation and polymer degradation), while three stages were observed for films with added glycerol (water loss, plasticizer degradation, and polymer degradation).

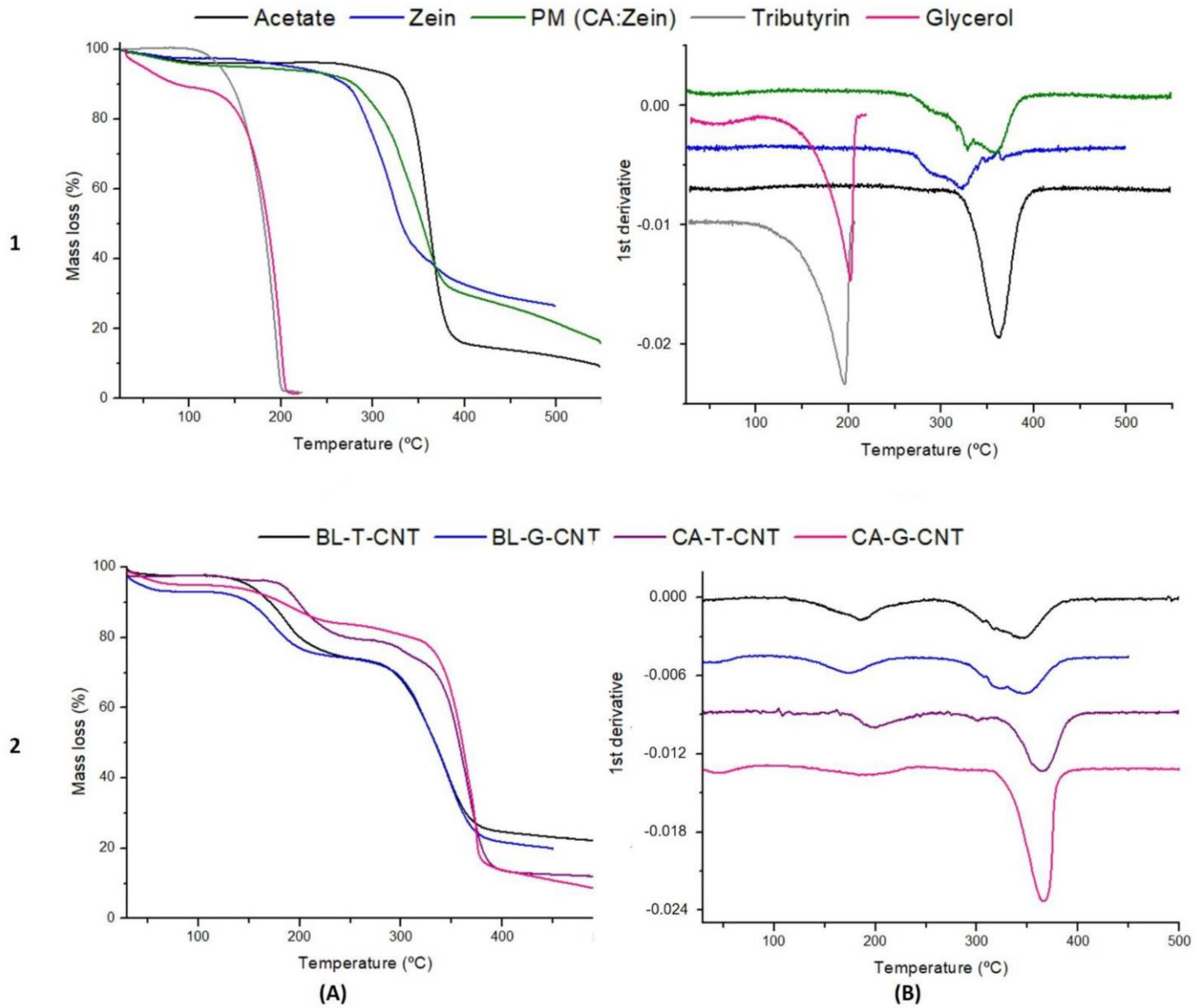

Figure 3. Thermogravimetric curves (**A**) and their respective 1st derivative (**B**) of: (1) pristine polymers (cellulose acetate and zein) and their physical mixture (PM), plus pristine plasticizers (tributyrin and glycerol); (2) control blends with tributyrin (BL-T-CNT) or glycerol (BL-G-CNT) and cellulose acetate films with tributyrin (CA-T-CNT) or glycerol (CA-G-CNT).

3.4. Mechanical and Water Vapor Barrier Properties

The blends' compatibility can also be evaluated from the quality of the polymer mixing states, and classified as synergism, additivity, or incompatibility [37,38]. Through the mechanical analysis, it was observed that the TS, YM, and E% parameters of the blends were lower than those of CA films, as displayed in Table 2. This behavior is justified by the additivity rule, in which the properties exhibited by the mixed material corresponded with the average properties of isolated components. In this case, the addition of a polymer to another does not entail positive (synergism) or negative (incompatibility) changes to the polymers. It needs to be emphasized that pure zein films, with or without plasticizers, were brittle and difficult to handle, which hindered the obtainment of the specimens required for both the mechanical and permeability assays. The blends with added tributyrin, in turn, were more flexible, allowing the samples to be characterized. Although blends with added glycerol were also more flexible than zein films, the presence of macro-holes and tears on

the films' surface (Figure 1) impaired the obtainment of specimens for the conduction of these assays.

Table 2. Thickness, mechanical properties (tensile strength, TS, elongation at break, E, and Young's modulus, YM), and water vapor permeability (WVP) of blends (BL) and control films (CA) plasticized with tributyrin (T) or glycerol (G) and with incorporated garlic essential oil (GEO), β-cyclodextrin (βCD) or inclusion complex (IC).

Sample	Thickness (μm)	TS (MPa)	E (%)	YM (Mpa)	WVP (10^{-10} g·Pa^{-1}·s^{-1}·m^{-1})
BL-T-CNT	121.6 (7.8) abc	4.7 (0.5) a	3.3 (0.4) a	313 (6) a	11.9 (1.3) c
BL-T- βCD	136.7 (18.1) abc	5.1 (0.3) a	2.6 (0.1) a	306 (39) a	11.8 (0.6) c
BL-T-GEO	136.2 (18.5) abc	5.9 (0.8) a	2.7 (0.1) a	338 (16) a	14.0 (1.2) c
BL-T-IC	250.8 (83.4) d	5.3 (0.5) a	3.3 (0.3) a	283 (33) a	27.6 (3.8) d
CA-T-CNT	58.8 (4.3) a	28.9 (4.9) c	7.7 (0.8) b	1203 (203) b	4.7 (0.2) a
CA-T-βCD	112.4 (46.0) abc	16.1 (5.5) b	2.8 (0.4) a	969 (287) b	10.8 (0.7) bc
CA-T-GEO	66.7 (13.1) a	29.1 (3.1) c	6.9 (0.4) b	1273 (97) b	6.5 (1.5) ab
CA-T-IC	155.9 (48.2) bc	7.7 (1.7) a	3.6 (0.5) a	389 (52) a	12.3 (1.9) c
BL-G-CNT	122.2 (5.8) abc	np	np	np	np
BL-G- βCD	180.2 (8.8)	np	np	np	np
BL-G-GEO	152.2 (4.2) bc	np	np	np	np
BL-G-IC	258.5 (49) d	np	np	np	np
CA-G-CNT	59.4 (0.9) a	np	np	np	np
CA-G- βCD	111 (3.6) abc	np	np	np	np
CA-G-GEO	76.8 (4) ab	np	np	np	np
CA-G-IC	182.6 (23.5) cd	np	np	np	np

np: not performed due to their high number of defects, restricting the obtaining of specimens in the dimensions required by the methodologies [25,26]. Means are followed by the standard deviation between parentheses. Mean values followed by the same letter, within the same column, are not significantly different according to Tukey's test ($p > 0.05$).

Besides this, the incorporation of IC or βCD into CA films significantly reduced TS, YM, and E% parameters compared with the control and the film containing GEO. This is justified by the insertion of defects in the matrix and interruption of secondary interactions between polymer chains [39]. However, the same effect was not observed when comparing the mechanical performance among the blends. This suggests that IC and βCD did not impair the structural cohesion between the polymers in the blend.

The elaborated CA:zein blends also underperformed compared with the CA control and GEO films at WVP (Table 2), probably due to their more porous nature when compared with the more solid appearance of the CA films (Figure 2). The presence of IC or βCD also impaired the water vapor barrier property of the films, making them more permeable than the controls. According to Oliveira et al. [3], a film's thickness heterogeneity may lead to problems with mechanical and barrier properties, which, in fact, was verified herein, since the films presenting the most irregular surfaces performed significantly worse on these assays.

WVP and mechanical properties are important parameters that must be considered when choosing an appropriate packaging for food. WVP, for example, is crucial for food preservation, while TS refers to material endurance and resilience. Although hydrophobic polymers, such as zein and CA, act as a better water vapor barrier than the hydrophilic ones, they are still less effective than the conventional plastics [40,41]. The mechanical properties of the biopolymers evaluated, measured in terms of TS and YM, need to be improved to achieve petrochemical polymer performance. Features such as brittleness, stiffness, and fragility may limit or even prevent their application [16,42]. To overcome these problems, several strategies are proposed, such as the investigation of new polymer nanocomposite-based films [5,14], incorporation of plasticizers [4,17], and mixing two or more polymers aiming for the obtainment of altered materials [15].

In the present work, we verified that the blends resulting from the mixing of zein and CA with tributyrin, despite underperforming compared with the CA control films, showed improvements when compared with the zein films. Incorporation of the nanoparticles βCD and IC impaired the film appearance and performance, while the addition of non-complexed GEO did not affect the films' properties. Although the direct incorporation of EOs into polymer matrices is not recommended, IC incorporation harmed the films' performance. Perhaps the choice of a natural βCD may not have been the best due to its insolubility in several organic solvents, such as acetone and ethanol, the solvents used for the filmogenic dispersion preparation [43]. Maybe a derivative CD with a hydrophobic nature or a higher solubility in polar organic solvents would solve the problem [43,44].

We also investigated two kinds of plasticizers: glycerol, widely used to plasticize biopolymer films, and tributyrin, a glycerol ester with three butyric acids of natural occurrence in milkfat [4,17,35,45]. It was observed that the plasticizer choice had an impact on the CA-zein blends. Glycerol has been incorporated into hydrophobic CA-films, as reported by Dias et al. [5], Gonçalves et al. [4] and Teixeira et al. [17]. However, its polar nature may have been the cause of the poor compatibility with the polymeric matrice blends, CA and zein, as verified by SEM micrographs and TG curves. Opposite behavior was observed when tributyrin was added as a plasticizer, resulting in films with a better performance and a more homogeneous appearance.

3.5. Antibacterial Investigation

S. aureus is an important foodborne pathogen, being considered one of the most significant threats to public health [46]. This bacterium is often responsible for foodborne intoxications through the production of heat-stable enterotoxins in various food products [47]. On the other hand, *L. innocua* has been used by many researchers as a surrogate for *Listeria monocytogenes* (considered a significant causative agent responsible for severe diseases in both humans and animals) in many food systems [48,49]. Therefore, both microorganisms were chosen to evaluate IC and GEO antibacterial activity. IC and GEO exhibited inhibitory activity against both bacteria, although the GEO antibacterial properties stood out (Table 3). However, it is essential to emphasize that the amount of EO present in IC corresponds to around 10% of the total IC weight (approximately 480 $\mu g \cdot mL^{-1}$), thus reducing the discrepancy between the MIC values found for them.

Table 3. Garlic essential oil (GEO) and inclusion complex (IC) minimal inhibitory concentration (MIC) against *S. aureus* and *L. innocua* after incubation at 37 °C for 24 h.

Bacteria	MIC ($\mu g \cdot mL^{-1}$)	
	GEO	**IC**
S. aureus	78.12	4800
L. innocua	156.25	4800

MIC values also indicated that *S. aureus* was more susceptible to the GEO antibacterial effect than *L. innocua*. One of the main action mechanisms of GEO is altering the permeability of the cell membrane due to the hydrophobic nature of the compounds [50,51] Therefore, the higher GEO effect in *S. aureus* than *L. innocua* can be related to the microorganisms' composition surface. *Listeria* sp. are Gram-positive bacteria; in spite of this, the microorganism has a peptidoglycan structure similar to Gram-negative bacteria, such as *E. coli* [52]. Thus, the greater hydrophilicity of the surface probably acted as a barrier to the EOs' components [52,53].

Regarding the films, their antibacterial activity was evaluated by the indirect contact methodology, also using *S. aureus* and *L. innocua* as target microorganisms at their optimal growth temperature (37 °C). Furthermore, *L. innocua* was tested under refrigeration conditions (7 °C) since this microorganism has the ability to grow under refrigeration. The polymer matrix did not exert significative influence on the antibacterial properties of

the films, and a similar pattern was observed when evaluating CA films and the blends. However, the kind of plasticizer used and the complexation or not of EO compounds did influence the outcomes. The results are displayed in Figure 4.

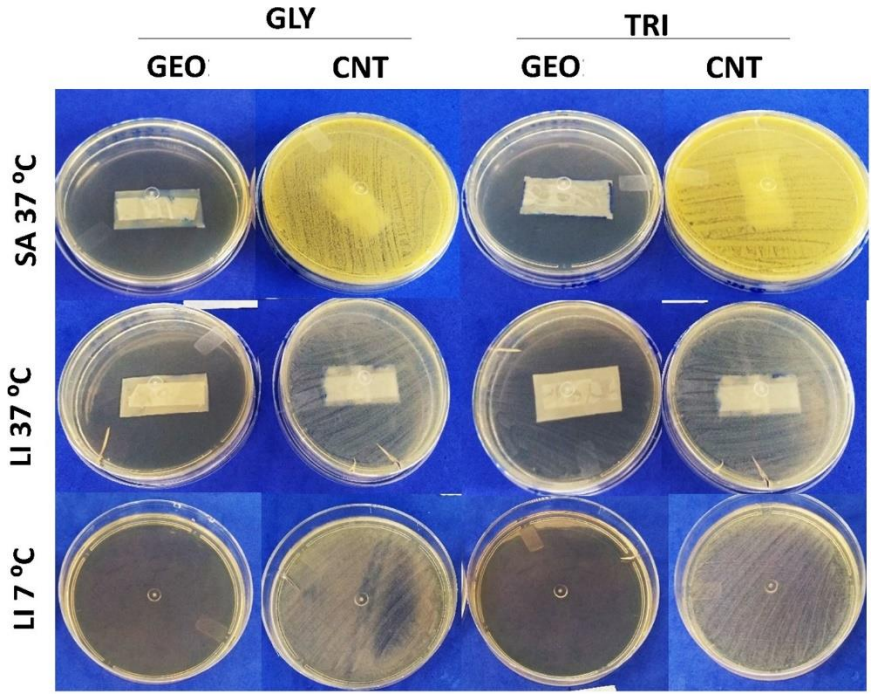

Figure 4. Antibacterial properties of active cellulose acetate films with 10% garlic essential oil incorporated (GEO) and control films (CNT), produced with glycerol (GLY) and tributyrin (TRI) as plasticizers, tested by indirect contact against *S. aureus* (SA) and *L. innocua* (LI) at 37 °C/24 h and 7 °C/10 day.

The plasticized films with incorporated GEO completely inhibited the growth of *S. aureus* after 24 h at 37 °C. On the other hand, differences in the kind of plasticizer were observed in *L. innocua* growth, tested under the same conditions. The active films produced with tributyrin (BL-T-GEO and CA-T-GEO) only partially inhibited the target bacteria, while the films with added glycerol completely inhibited *L. innocua* growth. The plasticized films containing the IC, in turn, did not affect bacteria growth, showing a similar outcome to the control films.

The differences found for plasticizer type can be attributed to the hydrophobic character of tributyrin [35]. This non-polar profile of tributyrin may enhance the entrapment of the GEO into the film matrix and, therefore, reduce the release of antibacterial agents. As a result, the films produced with this plasticizer exhibited lower antibacterial performance during the tests. Corroborating with this hypothesis, the GEO MIC results, previously discussed, indicated higher susceptibility of *S. aureus* to GEO components, which may explain the complete inhibition achieved with the active film; meanwhile, *L. innocua* exhibited a certain resistance, being partially inhibited.

Under refrigeration (7 °C/10 day), *L. innocua*, a psychrotrophic bacteria, did not exhibit visual growth when incubated in the presence of films with 10% GEO incorporated, independent of the plasticizer (Figure 4). In this case, despite the ability to grow under refrigeration temperatures [54], the cold conditions contributed to the GEO antibacterial activity. GEO thermal stability at lower temperatures was not assessed in the present research; however, low temperatures were already associated with stabilizing some GEO compounds [55]. This improved activity minimized the possible entrapment effect of tributyrin, and the films were able to control the bacteria growth during the incubation period. In addition, films with IC incorporated once again underperformed compared

with the films with added GEO and only partially inhibited *L. innocua* growth when under refrigerated conditions (results not shown). These results are in agreement with the MIC values found, since it was verified that a much higher concentration of IC was necessary to inhibit microbial growth, indicating that more IC should be added to the filmogenic dispersion in order to obtain films with a similar active property to the films with added GEO. However, this would hardly be viable.

4. Conclusions

In the present work, CA:zein active blends were successfully manufactured by the incorporation of GEO, as the bioactive agent, and tributyrin, as the plasticizer, into bio-based polymeric matrices. Despite the blends underperforming compared with the CA control films, they showed considerable improvements over zein films, which were brittle and fragile to the extent of impairing their manipulation. This could open a wider range of applications of zein as a food packaging component. Besides this, the results indicated that the films elaborated with non-complexed GEO could be used as a potential ally in food preservation, assisting in maintaining the microbiological quality and safety of food products. Films with IC incorporated, on the other hand, underperformed compared with those with added GEO regarding antibacterial activity.

Supplementary Materials: The following supporting information can be downloaded at: https://www.mdpi.com/article/10.3390/polysaccharides3010016/s1, Figure S1. Cellulose acetate and zein blends prepared with different polymer ratios (wt/wt). Figure S2. Cellulose acetate and zein as pellets and films. Figure S3. Thermogravimetric (TG) curves and their derivative (DTG) of βCD, inclusion complex (IC), garlic essential oil (GEO), and physical mixture (PM). * The red arrow indicates GEO loss in the inclusion complex. Figure S4. X-ray diffractograms of βCD, inclusion complex (IC), and physical mixture (PM). * Black arrows indicate the characteristic peaks for βCD. Figure S5. Thermogravimetric (TG) curves and their derivative (DTG) of cellulose acetate (CA) films and CA:zein blends incorporated with tributyrin (T) or glycerol (G) as plasticizers, and garlic essential oil (GEO), β-cyclodextrin (βCD), or inclusion complex (IC).

Author Contributions: Conceptualization, C.S.M. and N.d.F.F.S.; methodology, C.S.M., R.R.A.S., and A.L.V.F.; validation, C.S.M. and R.R.A.S.; investigation, C.S.M.; resources, N.d.F.F.S.; writing—original draft preparation, C.S.M., R.R.A.S., and T.R.A.; writing—review and editing, C.S.M. and T.V.d.O.; supervision, M.V.D., A.R.F.M., M.C.D.V., and N.d.F.F.S.; project administration, N.d.F.F.S.; funding acquisition, N.d.F.F.S. All authors have read and agreed to the published version of the manuscript.

Funding: This research was funded by the National Council for Scientific and Technological Development (grant number 142564/2018-4). In addition, this study was financed in part by the Coordenação de Aperfeiçoamento de Pessoal de Nível Superior—Brasil (CAPES)—Finance code 001.

Institutional Review Board Statement: Not applicable.

Informed Consent Statement: Not applicable.

Acknowledgments: The authors are grateful to colleagues from the Food Packaging Laboratory of Federal University of Viçosa (UFV), for exchange of experiences and knowledge, and to the Physics Department (UFV) for the use of experimental facilities. They also would like to thank Rhodia Solvay Group, for donating cellulose acetate, and Flo Chemical Corp, for donating zein.

Conflicts of Interest: The authors declare no conflict of interest.

References

1. Kato, L.S.; Conte-Junior, C.A. Safety of plastic food packaging: The challenges about non-intentionally added-substances (NIAS) discovery, identification and risk assessment. *Polymers* **2021**, *13*, 2077. [CrossRef] [PubMed]
2. Mangaraj, S.; Yadav, A.; Bal, L.M.; Dash, S.K.; Mahanti, N.K. Application of Biodegradable Polymers in Food Packaging Industry: A Comprehensive Review. *J. Packag. Technol. Res.* **2019**, *3*, 77–96. [CrossRef]
3. Oliveira, T.V.; Freitas, P.A.V.; Pola, C.C.; Silva, J.O.R.; Diaz, L.D.A.; Ferreira, S.O.; Soares, N.F.F. Development and optimization of antimicrobial active films produced with a reinforced and compatibilized biodegradable polymers. *Food Packag. Shelf. Life* **2020**, *24*, 100459. [CrossRef]

4. Gonçalves, S.M.; Santos, D.C.; Motta, J.F.G.; Santos, R.R.; Chávez, D.W.H.; Melo, N.R. Structure and functional properties of cellulose acetate incorporated with glycerol. *Carbohydr. Polym.* **2019**, *209*, 190–197. [CrossRef] [PubMed]
5. Dias, M.V.; Sousa, M.M.; Lara, B.R.B.; Azevedo, V.M.; Soares, N.F.F.; Borges, S.V.; Queiroz, F. Thermal and morphological properties and kinetics of diffusion of antimicrobial films on food and a simulant. *Food Packag. Shelf. Life* **2018**, *16*, 15–22. [CrossRef]
6. Pola, C.C.; Medeiros, E.A.A.; Pereira, O.L.; Souza, V.G.L.; Otoni, C.G.; Camilloto, G.P.; Soares, N.F.F. Cellulose acetate active films incorporated with oregano (*Origanum vulgare*) essential oil and organophilic montmorillonite clay control the growth of phytopathogenic fungi. *Food Packag. Shelf. Life* **2016**, *9*, 69–78. [CrossRef]
7. Malm, M.; Liceaga, A.M.; San Martin-Gonzalez, F.; Jones, O.G.; Garcia-Bravo, J.M.; Kaplan, I. Development of Chitosan Filmsfrom Edible Crickets and Their Performance as a Bio-Based Food Packaging Material. *Polysaccharides* **2021**, *2*, 744–758. [CrossRef]
8. Atta, O.M.; Manan, S.; Shahzad, A.; Ul-Islam, M.; Ullah, M.W.; Yang, G. Biobased materials for active packaging: A review. *Food Hydrocoll.* **2022**, *125*, 107419. [CrossRef]
9. Atta, O.M.; Manan, S.; Ul-Islam, M.; Ahmed, A.A.Q.; Ullah, M.W.; Yang, G. Development and characterization of plant oil-incorporated carboxymethyl cellulose/bacterial cellulose/glycerol-based antimicrobial edible films for food packaging applications. *Adv. Compos. Hybrid. Mater.* **2022**, 1–17. [CrossRef]
10. Yuvarai, D.; Iyyappan, J.; Gnanasekaran, R.; Ishwarya, G.; Harshini, R.P.; Dhithya, V.; Chandran, M.; Kanishka, V.; Gomathi, K. Advances in bio food packaging—An overview. *Heliyon* **2021**, *7*, e07998. [CrossRef] [PubMed]
11. Aytac, Z.; Huang, R.; Vaze, N.; Xu, T.; Eitzer, B.D.; Krol, W.; MacQueen, K.A.; Chang, H.; Bousfield, D.W.; Chan-Park, M.B.; et al. Development of Biodegradable and Antimicrobial Electrospun Zein Fibers for Food Packaging. *ACS Sustain. Chem. Eng.* **2020**, *8*, 15354–15365. [CrossRef]
12. US Food and Drug Administration. Available online: https://www.cfsanappsexternal.fda.gov/scripts/fdcc/index.cfm?set=FCN&id=2043&sort=FCN_No&order=DESC&startrow=1&type=basic&search=cellulose%20acetate (accessed on 20 January 2022).
13. US Food and Drug Administration. Available online: https://www.accessdata.fda.gov/scripts/cdrh/cfdocs/cfcfr/CFRSearch.cfm?fr=184.1984 (accessed on 20 January 2022).
14. Lara, B.R.B.; Andrade, P.S.; Guimarães Junior, M.; Dias, M.V.; Alcântara, L.A.P. Novel Whey Protein Isolate/Polyvinyl Biocomposite for Packaging: Improvement of Mechanical and Water Barrier Properties by Incorporation of Nano-silica. *J. Polym. Environ.* **2021**, *29*, 2397–2408. [CrossRef]
15. Moraes, A.R.F.; Pola, C.C.; Bilck, A.P.; Yamashita, F.; Tronto, J.; Medeiros, E.A.A.; Soares, N.F.F. Starch, cellulose acetate and polyester biodegradable sheets: Effect of composition and processing conditions. *Mater. Sci. Eng. C* **2017**, *78*, 932–941. [CrossRef]
16. Sanyang, M.L.; Sapuan, S.M.; Jawaid, M.; Ishak, M.R.; Sahari, J. Effect of plasticizer type and concentration on physical properties of biodegradable films based on sugar palm (*Arenga pinnata*) starch for food packaging. *J. Food Sci. Technol.* **2016**, *53*, 326–336. [CrossRef] [PubMed]
17. Teixeira, S.C.; Silva, R.R.A.; Oliveira, T.V.; Stringheta, P.C.; Pinto, M.R.M.; Soares, N.F.F. Glycerol and triethyl citrate plasticizer effects on molecular, thermal, mechanical, and barrier properties of cellulose acetate films. *Food Biosci.* **2021**, *42*, 101202. [CrossRef]
18. Arruda, T.R.; Marques, C.S.; Soares, N.F.F. Native Cyclodextrins and Their Derivatives as Potential Additives for Food Packaging: A Review. *Polysaccharides* **2021**, *2*, 825–842. [CrossRef]
19. Ayala-Zavala, J.F.; González-Aguilar, G.A. Optimizing the use of garlic oil as antimicrobial agent on fresh-cut tomato through a controlled release system. *J. Food Sci.* **2010**, *75*, M398–M405. [CrossRef] [PubMed]
20. Marques, C.S.; Carvalho, S.G.; Bertoli, L.D.; Villanova, J.C.O.; Pinheiro, P.F.; dos Santos, D.C.M.; Yoshida, M.I.; Freitas, J.C.C.; Cipriano, D.F.; Bernardes, P.C. β-Cyclodextrin inclusion complexes with essential oils: Obtention, characterization, antimicrobial activity and potential application for food preservative sachets. *Food Res. Int.* **2019**, *119*, 499–509. [CrossRef] [PubMed]
21. Mukurumbira, A.R.; Shellie, R.A.; Keast, R.; Palombo, E.A.; Jadhav, S.R. Encapsulation of essential oils and their application in antimicrobial active packaging. *Food Control* **2022**, *136*, 108883. [CrossRef]
22. Ali, S.; Khatri, Z.; Oh, K.W.; Ki, I.S.; Kim, S.H. Zein/cellulose acetate hybrid nanofibers: Electrospinning and characterization. *Macromol. Res.* **2014**, *22*, 971–977. [CrossRef]
23. Liu, F.; Li, X.; Wang, L.; Yan, X.; Ma, D.; Liu, Z.; Liu, X. Sesamol incorporated cellulose acetate-zein composite nanofiber membrane: As efficient strategy to accelerate diabetic wound healing. *Int. J. Biol. Macromol.* **2020**, *149*, 627–638. [CrossRef]
24. Hill, L.E.; Gomes, C.; Taylor, T.M. Characterization of beta-cyclodextrin inclusion complexes containing essential oils (trans-cinnamaldehyde, eugenol, cinnamon bark, and clove bud extracts) for antimicrobial delivery application. *LWT-Food Sci. Technol.* **2013**, *51*, 86–93. [CrossRef]
25. ASTM. *ASTM D882-12*; Standard Test Method for Tensile Properties of Thin Plastic Sheeting. ASTM: West Conshohocken, PA, USA, 2012.
26. ASTM. *ASTM E96/E96M-10*; Standard Test Method for Water Vapor Transmission of Materials. ASTM: West Conshohocken, PA, USA, 2010.
27. CLSI. *Methods for Dilution Antimicrobial Susceptibility Tests for Bacteria That Grow Aerobically*, 9th ed.; CLSI: Wayne, PA, USA, 2012.
28. R Core Team. *R: A Language and Environment for Statistical Computing*; R Foundation for Statistical Computing: Vienna, Austria, 2021; Available online: https://www.R-project.org/ (accessed on 20 December 2021).
29. Santos, E.H.; Kamimura, J.A.; Hill, L.E.; Gomes, C.L. Characterization of carvacrol beta-cyclodextrin inclusion complexes as delivery systems for antibacterial and antioxidant applications. *LWT-Food Sci. Technol.* **2015**, *60*, 583–592. [CrossRef]

30. Giordano, F.; Novak, C.; Moyano, J.R. Thermal analysis of cyclodextrins and their inclusion compounds. *Thermochim. Acta* **2001**, *380*, 123–151. [CrossRef]
31. Piletti, R.; Zanetti, M.; Jung, G.; Melo, J.M.M.; Dalcanton, F.; Soares, C.; Riella, H.G.; Fiori, M.A. Microencapsulation of garlic oil by β-cyclodextrin as thermal protection method for antibacterial action. *Mater. Sci. Eng. C* **2019**, *94*, 139–149. [CrossRef] [PubMed]
32. Abarca, R.L.; Rodríguez, F.J.; Guarda, A.; Galotto, M.J.; Bruna, J.E. Characterization of beta-cyclodextrin inclusion complexes containing an essential oil component. *Food Chem.* **2016**, *196*, 968–975. [CrossRef] [PubMed]
33. Narayanan, G.; Boy, R.; Gupta, B.S.; Tonelli, A.E. Analytical techniques for characterizing cyclodextrins and their inclusion complexes with large and small molecular weight guest molecules. *Polym. Test.* **2017**, *62*, 402–439. [CrossRef]
34. Takahashi, A.I.; Veiga, F.J.B.; Ferraz, H.G. A literature review of cyclodextrin inclusion complexes characterization—Part II: X-ray diffraction, infrared spectroscopy and nuclear magnetic resonance. *Int. J. Pharm. Sci. Rev. Res.* **2012**, *1*, 8–15.
35. Iglesias Montes, M.L.; D'amico, D.A.; Manfredi, L.B.; Cyras, V.P. Effect of Natural Glyceryl Tributyrate as Plasticizer and Compatibilizer on the Performance of Bio-Based Polylactic Acid/Poly(3-Hydroxybutyrate) Blends. *J. Polym. Environ.* **2019**, *27*, 1429–1438. [CrossRef]
36. Freitas, P.A.V.; Silva, R.R.A.; Oliveira, T.V.; Soares, R.R.A.; Junior, N.S.; Moraes, A.R.F.; Pires, A.C.S.; Soares, N.F.F. Development and characterization of intelligent cellulose acetate-based films using red cabbage extract for visual detection of volatile bases. *LWT-Food Sci. Technol.* **2020**, *132*, 109780. [CrossRef]
37. Meister, J. *Polymer Modification: Principles, Techniques and Applications*, 1st ed.; CRC Press: Boca Raton, FL, USA, 2000; 914p.
38. Shanks, R.A. Concepts and classification of compatibilization processes. In *Compatibilization of Polymer Blends*, 1st ed.; Ajitha, A.R., Thomas, S., Eds.; Elsevier: Amsterdam, The Netherlands, 2020; pp. 31–56.
39. Callister, W.D., Jr.; Rethwisch, D.G. *Materials Science and Engineering: An Introduction*, 8th ed.; John Willey & Sons: Hoboken, NJ, USA, 2010; 992p.
40. Farhan, A.; Hani, N.M. Characterization of edible packaging films based on semi-refined kappa-carrageenan plasticized with glycerol and sorbitol. *Food Hydrocoll.* **2017**, *64*, 48–58. [CrossRef]
41. Togashi, Y.; Hara, M. Water vapor permeability of polypropylene. *Fusion Sci. Technol.* **2011**, *60*, 1471–1474. [CrossRef]
42. Hazrol, M.D.; Sapuan, S.M.; Zainudin, E.S.; Zuhri, M.Y.M.; Abdul Wahab, N.I. Corn Starch (*Zea mays*) Biopolymer Plastic Reaction in Combination with Sorbitol and Glycerol. *Polymers* **2021**, *13*, 242. [CrossRef] [PubMed]
43. Miranda, J.C.; Martins, T.E.A.; Veiga, F.; Ferraz, H.G. Cyclodextrins and ternary complexes: Technology to improve solubility of poorly soluble drugs. *Braz. J. Pharm. Sci.* **2011**, *47*, 665–681. [CrossRef]
44. Przybyla, M.A.; Yilmaz, G.; Becer, R. Natural cyclodextrins and their derivatives for polymer synthesis. *Polym. Chem.* **2020**, *11*, 7582–7602. [CrossRef]
45. Vazquez, R.; Nogueira, R.; Orfão, M.; Mata, J.L.; Saramago, B. Stability of triglyceride liquid films on hydrophilic and hydrophobic glasses. *J. Colloid Interface Sci.* **2006**, *299*, 274–282. [CrossRef] [PubMed]
46. Rubab, M.; Shahbaz, H.M.; Olaimat, A.N.; Oh, D.H. Biosensors for Rapid and Sensitive Detection of *Staphylococcus aureus* in Food. *Biosens. Bioelectron.* **2018**, *105*, 49–57. [CrossRef] [PubMed]
47. Hennekinne, J.A.; De Buyser, M.L.; Dragacci, S. *Staphylococcus aureus* and Its Food Poisoning Toxins: Characterization and Outbreak Investigation. *FEMS Microbiol. Rev.* **2012**, *36*, 815–836. [CrossRef] [PubMed]
48. Shamloo, E.; Hosseini, H.; Moghadam, A.Z.; Larsen, H.M.; Haslberger, A.; Alebouyeh, M. Importance of *Listeria Monocytogenes* in Food Safety: A Review of Its Prevalence, Detection, and Antibiotic Resistance. *Iran. J. Vet. Res.* **2019**, *20*, 241–254. [PubMed]
49. Friedly, E.C.; Crandall, P.G.; Ricke, S.; O'Bryan, C.A.; Martin, E.M.; Boyd, L.M. Identification of *Listeria Innocua* Surrogates for *Listeria Monocytogenes* in Hamburger Patties. *J. Food Sci.* **2008**, *73*, 174–178. [CrossRef] [PubMed]
50. Münchberg, U.; Anwar, A.; Mecklenburg, S.; Jacob, C. Polysulfides as Biologically Active Ingredients of Garlic. *Org. Biomol. Chem.* **2007**, *5*, 1505–1518. [CrossRef] [PubMed]
51. Arbach, M.; Santana, T.M.; Moxham, H.; Tinson, R.; Anwar, A.; Groom, M.; Hamilton, C.J. Antimicrobial Garlic-Derived Diallyl Polysulfanes: Interactions with Biological Thiols in *Bacillus Subtilis*. *Biochim. Biophys. Acta—Gen. Subj.* **2019**, *1863*, 1050–1058. [CrossRef] [PubMed]
52. Bierne, H.; Cossart, P. *Listeria Monocytogenes* Surface Proteins: From Genome Predictions to Function. *Microbiol. Mol. Biol. Rev.* **2007**, *71*, 377–397. [CrossRef] [PubMed]
53. Fiedler, F. Biochemistry of the Cell Surface of Listeria Strains: A Locating General View. *Infection* **1988**, *16*, S92–S97. [CrossRef] [PubMed]
54. Sheng, L.; Shen, X.; Su, Y.; Xue, Y.; Gao, H.; Mendoza, M.; Green, T.; Hanrahan, I.; Zhu, M.-J. Effects of 1-Methylcyclopropene and Gaseous Ozone on *Listeria Innocua* Survival and Fruit Quality of Granny Smith Apples during Long-Term Commercial Cold Storage. *Food Microbiol.* **2022**, *102*, 103922. [CrossRef] [PubMed]
55. Fujisawa, H.; Suma, K.; Origuchi, K.; Seki, T.; Ariga, T. Thermostability of Allicin Determined by Chemical and Biological Assays. *Biosci. Biotechnol. Biochem.* **2008**, *72*, 2877–2883. [CrossRef] [PubMed]